

Available online at www.sciencedirect.com**ScienceDirect**

Physics Procedia 83 (2016) 532 – 539

Physics

Procedia9th International Conference on Photonic Technologies - LANE 2016

Mechanical properties of laser-jetted SAC305 solder on coated optical surfaces

Max Mäusezahl^a, Marcel Hornaff^a, Thomas Burkhardt^a, Erik Beckert^{a,*}^a*Fraunhofer Institute for Applied Optics and Precision Engineering, Albert-Einstein-Strasse 7, 07745 Jena, Germany*

Abstract

Micro-optical packaging methods using laser-based Solderjet Bumping are a versatile alternative to established adhesive bonding, featuring the advantages of metallic solder in optical systems. Yet, aging properties have often been studied only for certain use cases. To examine application independent, long-term material properties of SAC305, square substrates of two widely used soda-lime glasses and the ceramic Al_2O_3 have been coated with a thin metallic layer system to be receptive for metallic solder. Using Solderjet Bumping, SAC305 balls of 400 μm diameter have been processed with different parameters to form an array of solder bumps on each substrate. While aging for two months at elevated temperature and for over a year at room temperature, shear strengths and failure modes of the individual bumps have been measured and compared. The results show that the mechanical stability of such bumps will stabilize on a level known from research by the electronics industry while observing a considerable dependency on the used substrate material.

© 2016 The Authors. Published by Elsevier B.V. This is an open access article under the CC BY-NC-ND license (<http://creativecommons.org/licenses/by-nc-nd/4.0/>).

Peer-review under responsibility of the Bayerisches Laserzentrum GmbH

Keywords: SAC305; Solderjet Bumping; micro-optics; shear strength testing; aging

1. Introduction

The ongoing miniaturisation of optical components and systems, with increased requirements towards high-precision alignment and long-term stability, challenge the limits of micro-optical assembly processes. Different organic adhesives have been under rapid development over the last decades and became the predominant choice of

* Corresponding author. Tel.: +49-3641-807-338 ; fax: +49 -3641-807-604 .
E-mail address: erik.beckert@iof.fraunhofer.de

the industry for such tasks. They, however, often fall short of some desirable properties known from metallic joints regarding long-term stability, radiation robustness and outgassing in vacuum environments, Beckert et al. (2008).

Metal-based soldering is a versatile alternative, offering several advantages over such adhesives. A solder joint is usually formed between the solder and one or more metallic surfaces using heat and pressure, creating new alloys on the contact surfaces which is called layer of intermetallic compounds (IMC). The wide use of a large variety of solder in the electronic industry due to its low cost, variable mechanical and excellent electrical properties lead to a well-known bonding system for a broad range of applications. After the restriction of lead usage for industrial applications due to environmental and health concerns, different promising solder systems like Sn-Ag-Cu (SAC) replaced the formerly used Sn-Pb solder alloys. Different variations of this system including 96.5Sn-3.0Ag-0.5Cu (SAC305), 95.5Sn-3.8Ag-0.7Cu (SAC387), 95.5Sn-3.9Ag-0.6Cu (SAC396) or 95.5Sn-4.0Ag-0.5Cu (SAC405) were proposed for their different strengths regarding melting temperature, solderability or surface wetting properties compared to other lead free solders, Ma et al. (2007).

The different effects of aging on solder joints were discussed early; namely solder joint fatigue being one of the most common failures in electronic packages after thermal cycling. It is well known that solder joints will constantly change on a microscopic and macroscopic level, usually losing an amount of their ultimate strength over time, Zhong and Yi (1998). This can be explained by formation of different microstructural alloys in the IMC, which can for example result in faster propagation of miniature cracks and eventually failure of the joint, Lampe (1976) and Chou (2002). One main difficulty hindering comparability and reusability for all work done in the field of characterizing solder are the manifold approaches to prepare test specimen that not only reflect a certain use case but true solder material properties. Former work is often based on standardized tensile bars which are big compared to the amount of solder necessary for junctions between micro-optical components like e.g. in Amagai et al. (2002) or Anderson and Haringa (2004). Because of the consequently lower heat capacities such junctions undergo e.g. faster cooling and possibly yield different characteristics.

Hybrid optical systems in particular bring some additional requirements since non-metallic optical materials as glass are usually not directly solderable. A possible way to achieve a solderable state is to coat a surface with a metallic layersystem which promotes wettability. This is done locally since opaque surfaces are not applicable in light beam paths. Also, additional tension in optical materials has to be avoided to prevent destruction or altering of optical properties. Laser-based Solderjet Bumping is a technology providing locally restricted energy input to prevent component damage whilst allowing precise and flexible positioning of miniature solder joints. These can also exhibit a significantly higher ultimate strength than solder joints from conventional reflow processes, Ding et al. (2012).

2. Experimental procedures

2.1. Solderjet Bumping and specimen preparation

Solderjet Bumping is a laser-based process, schematically shown in fig. 1(a), to precisely apply single solder bumps to a metallic surface originally developed for flip chip assembly. Preformed solder balls of diameters ranging from 40 μm to 760 μm and materials ranging from low-melting SnBi-SAC to high-melting AuSn, AuGe or AuSi alloys can be used. They are provided in a reservoir to be singularized and transported into a placing capillary. This capillary is conically formed at the tip, so that a single solder ball forced by applied nitrogen pressure will be held in place there. The capillary is then moved to the desired position where the solder bump should be applied e.g. by a six-axis robot or a gantry system. In this situation a focused laser pulse of width t_p and laser current I is used to reflow the solder. The nitrogen will eject the molten solder towards the substrate where a bond gets formed while also providing an inert atmosphere. On a flat surface and with a vertically positioned capillary a solder bump with roughly spherical cap geometry is formed. Precise wetting behavior depends on laser energy, nitrogen pressure and the surface wetting behavior.

Specimen design for a medium size aging experiment tackles two major problems: On one hand the sample size for a single data point has to be large enough to be statistically significant but small enough to allow a larger amount of different tested parameter sets. From previous experiments it was deduced that sample sizes bigger than 30 solder bumps are necessary to gain reproducible and significant mechanical results. For these reasons square substrates of 25 mm side length were produced to hold an array of seven times eight solder bumps (see fig. 1(b) and fig. 3(a)).

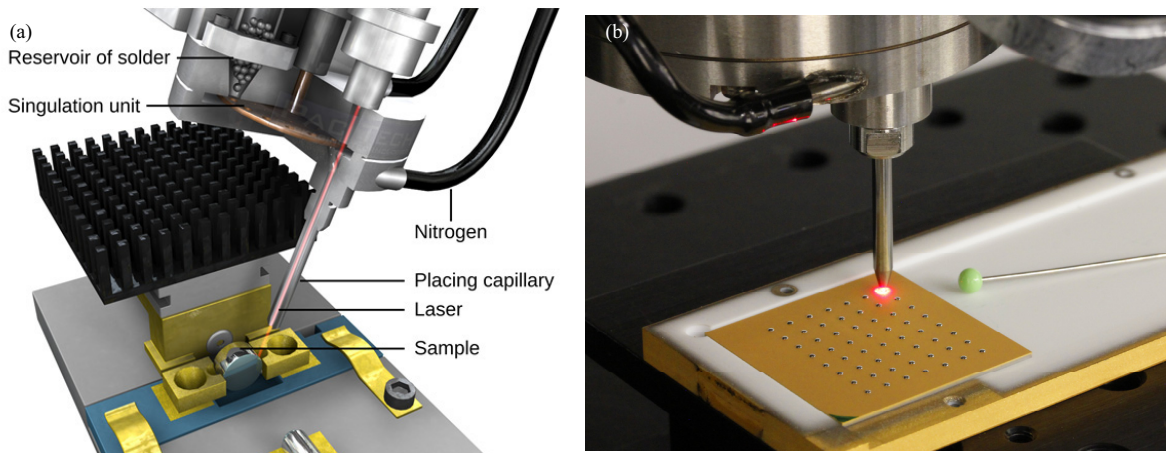


Fig. 1. The Solderjet Bumping process. (a) Schematic of the Solderjet bond head. (b) Photograph of the used setup showing the bond head with activated pilot laser for positioning and the specimen with a simple holding arrangement (pin head for scale).

In the presented study three different substrates were used: BOROFLOAT[®] 33 borosilicate glass by SCHOTT (1.1 mm thickness), plain microscope slides by the provider VWR (soda lime glass of 1.0 mm thickness) and an opaque but non-metallic Al₂O₃ ceramic (0.6 mm thickness). In preparation for the soldering process these were cleaned in a multistage aqueous, surfactant based cleaning process and then coated with a Ti-Pt-Au layersystem of less than 1 μm thickness in a DC magnetron sputtering process. In this state solder can be applied by Solderjet Bumping. Because of good availability and wide usage, SAC305 solder balls of 400 μm diameter were chosen and bumped vertically with 800 μm distance between capillary and substrate surface.

2.2. Aging and shear testing procedure

Directly after applying solder bumps the specimens were stored either in a dry air cupboard at room temperature or in an oven at 150 °C. Ball shear testing, as schematically shown in fig. 2(a), is a method routinely used to investigate mechanical strength of so called ball grid arrays (BGA). A force F , called shear load, is applied parallel to the

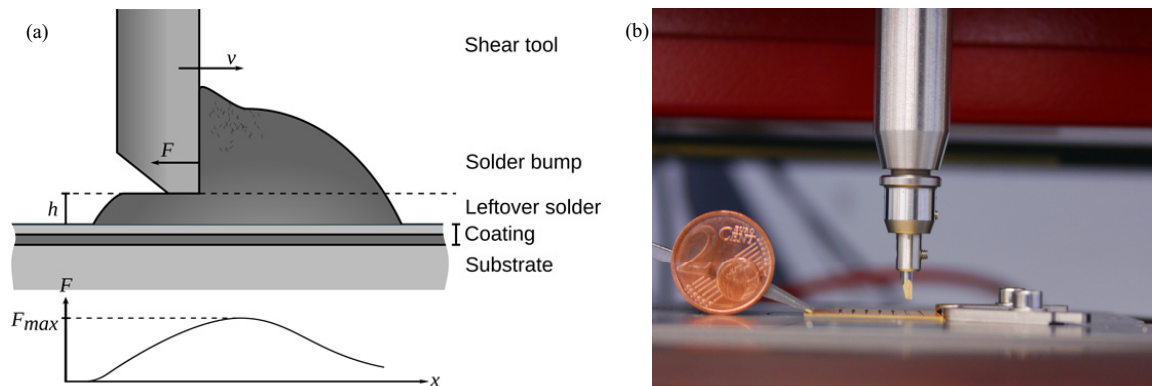


Fig. 2. Shear testing setup in detail. (a) Schematic of a ball shear test in progress. The maximum force is approximately reached at the centre of the solder bump. (b) Photograph of the setup used for this study. The shear tool is attached to a force measuring system above. The specimen is kept in place on a heated chuck at 25 °C by three metal clamps (two cent euro coin for scale).

surface under the substrate by a flat shear tool in height h while constantly moving with a velocity v , called shear rate, so that a single solder bump gets sheared off. The measurement yields a $F(x)$ force over way characteristic and leaves part of the solder of shear area A on the substrate. Approximately at the center of the bump the maximum shear load F_{max} is reached. The shear strength $\tau = F_{max}/A$ is often used as a material characteristic parameter, although it is known that τ depends on other shearing parameters like shear rate as well, Nakamori et al. (2002) and Chia et al. (2006). Sometimes the leftover solder forms no complete socket of circular shape if viewed from above. Instead the bump breaks off at some point leaving only part of this circle behind (see fig. 3). For this study a shear testing machine of type “Delvotec 5600 Pull/Sheartester” was used with a shear tool of 1.2 mm width at a shear rate of $50 \mu\text{m}\cdot\text{s}^{-1}$ and a defined substrate temperature of 25°C . The setup is shown in fig. 2(b). The shear area A of leftover solder was measured by automatically photographing the individual bumps as seen in fig. 3 and using programmatic image feature detection to measure their geometries.

3. Results and discussion

3.1. Shear testing and Solderjet Bumping parameters

First a series of experiments was performed to define parameters for the Solderjet Bumping and shear testing processes. Possible parameters were selected based on known behavior regarding bump geometry and damage to the substrates.

For sample sizes above 30 bumps the distribution of forces for otherwise identical processed bumps clearly began to show the characteristic of a normal distribution (fig. 4(a)). For such bumps it was, however, not possible to see any relation between the slight variations in size and the variation of measured shear loads (fig. 4(b)).

This indicates that the sample preparation was capable of producing a larger number of geometrically nearly

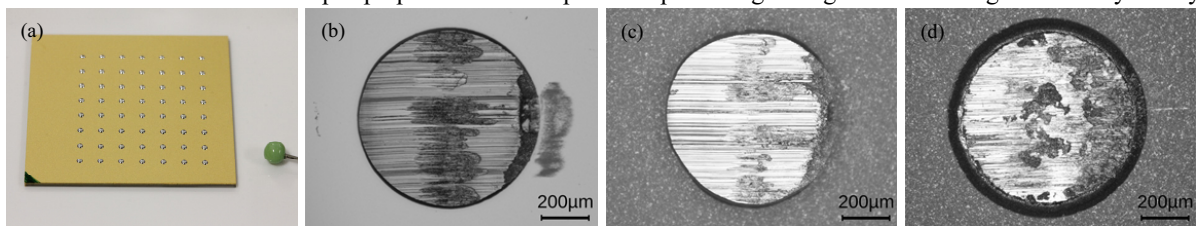


Fig. 3. (a) Square specimen of 25 mm side length with a seven times eight solder bump grid (2.5 mm pitch) were used. The clearance on the left side allows mounting in the shear tester (pin head for scale). (b),(c),(d) Top view light optical micrographs showing leftover solder after shear testing for BF33 substrate in (b), Al_2O_3 substrate in (c) and Al_2O_3 substrate after 20 days at 150°C in (d). The shear testing direction was left to right. The sample aged at elevated temperature shows a dark ring around the solder bump which might be a result of a metallic diffusion process.

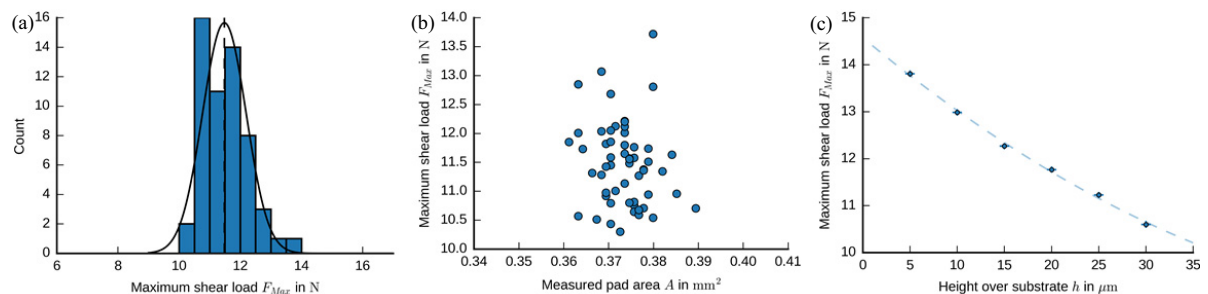


Fig. 4. (a) A typical distribution of maximum shear loads for one specimen with solder bumps from identical conditions in comparison with a normal distribution. (b) The relation between the measured pad area and shear load for the bumps of this specimen. (c) The relation between shear load and shear height for otherwise identical specimens and shear testing parameters. The dashed line marks a quadratic relation.

identical solder bumps so that other effects dominate the produced slight variation of measured shear loads. When changing the shear height, the shear area was affected accordingly (fig. 4(c)) and a quadratic relation between F_{max} and h could be measured while the shear strength $\tau(F_{max}, A(h))$ stayed nearly constant.

To perform shear tests, the geometry of the bumps should not be too flat so that the shear tool has enough area to apply a steady force on the bump. While the laser energy as the combined result of laser current and pulse width is not a perfect indicator, generally higher laser energy leads to flatter bump geometry because of increased wetting, Beckert et al. (2008). An investigation on coated soda lime glass showed that lower laser energies do not only lead to such flat geometries, but also produced bumps with higher shear strength as listed in table 1. This might be a result of varying formed microstructural SAC305 phases depending on used energy, heating time and cooling time. Finally a laser current of 60 A, pulse width of 2.5 ms for the glass substrates and a different laser current of 75 A, pulse width of 5 ms for Al_2O_3 (to produce similar geometries) as well as a shear height of $15\text{ }\mu\text{m}$ were used for the following experiments.

Table 1. Achieved shear strengths for different Solderjet Bumping parameters on coated microscopy slides (average over 56 solder bumps each).

Laser parameters current/pulse width	Measured laser energy in mJ	Diameter in μm	Shear strength in MPa (as soldered)	Shear strength in MPa (after 20 d)
50 A / 10 ms	540	962	23.6	20.3
60 A / 6 ms	490	992	23.8	19.7
75 A / 3 ms	378	1018	20.3	19.2
45 A / 8 ms	360	880	29.3	24.9
70 A / 2 ms	230	779	36.6	30.1
60 A / 2.5 ms	217	740	39.3	32.3

3.2. Effects of aging and elevated temperature aging

While aging at room temperature, the solder bumps didn't show visible changes under a light microscope. However the solder bumps aged at elevated temperature, but well below the melting point of SAC305 (near eutectic, solidus: 217°C , liquidus: 220°C , here: 150°C), exhibited two visible modifications. Firstly, a dark ring formed around the solder bump (see fig. 3(d)) which grew over time and reached a diameter more than 20 % larger than the solder bump itself after 30 days averagely. This might be due to an ongoing diffusion of Sn, Ag or Cu into the Au coating like it happens while the bonding and the IMC are created. Additional research is required to clarify this behavior. Secondly, the solder bumps usually looked shiny and smooth under a microscope. After 30 days aging under elevated temperature conditions they began to look "ragged" instead of smooth especially close to the substrate surface.

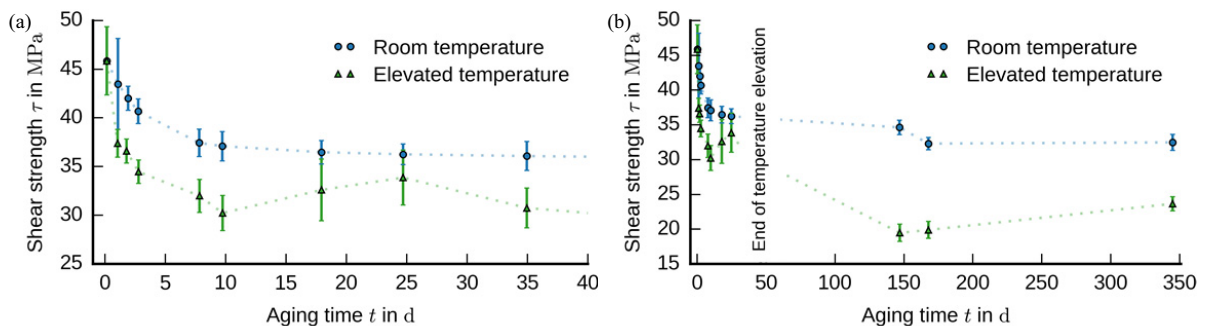


Fig. 5. Development of shear strengths of SAC305 on coated Al_2O_3 substrates for (a) the first days and (b) the whole experiment.

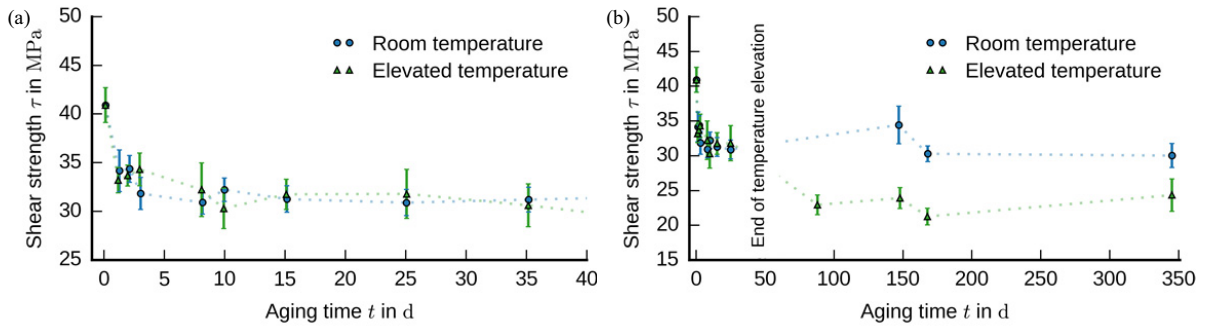


Fig. 6. Development of shear strengths of SAC305 on coated BF33 substrates for (a) the first days and (b) the whole experiment.

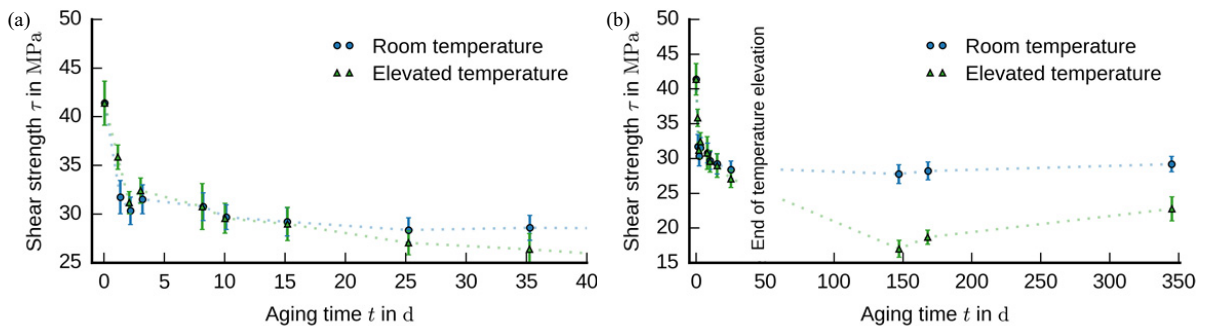


Fig. 7. Development of shear strengths of SAC305 on coated microscope slides as substrate for (a) the first days and (b) the whole experiment.

All bumps exhibited a high initial shear strength that decreased rapidly over the first 20 days. Afterwards the decrease was much slower. This can be explained by the development of micro-metallic alloys in the solder. Diffusion typically leads to growing grains of different phases in the metallic SAC system which alters resistance towards applied external forces, Lechovič et al. (2008). For the solder bumps on Al_2O_3 substrate, which had the highest initial shear strength in this experiment, the solder bumps aged under elevated temperature conditions had a constantly lower shear strength from the beginning (see fig. 5). After ending the temperature elevation phase and putting the remaining specimen from elevated to room temperature, there seemed to be an additional drop of shear strength in the following days.

The glass substrates also exhibited this drop (see fig. 6 and fig. 7), but the solder bumps which aged under elevated temperature showed no significantly different properties this point. This might occur, because the elevated temperature time was too short to cause noticeable structural modification in the first place, but introduced a long-term damage nevertheless. Also, the specimen which were under elevated temperature conditions generally exhibited a higher standard deviation of the shear strength for one specimen and a larger fluctuation between the measured shear strengths of two consecutive measurement times. The cause of this phenomenon could not be found, but might be the explanation for the overall, seemingly unsteady behavior of the measured shear strengths.

For all substrates the final shear strength of the solder bumps, which had initially been under elevated temperature conditions for 30 days, is about 20% lower than the shear strength of the solder bumps which had always been under room temperature conditions.

In the comparison in fig. 8 the three examined substrates behaved identical under room temperature conditions regarding the aging process and changes of shear strengths. However, they had different initial shear strengths. E.g. the shear strengths of solder bumps on Al_2O_3 were constantly higher than the shear strength of solder bumps on the two examined glasses. This might be due to the higher laser energy necessary to form bumps of identical size on Al_2O_3 in combination with the higher thermal conductivity of Al_2O_3 ($\approx 40 \text{ W} \cdot \text{m}^{-1} \cdot \text{K}^{-1}$) in comparison to the thermal

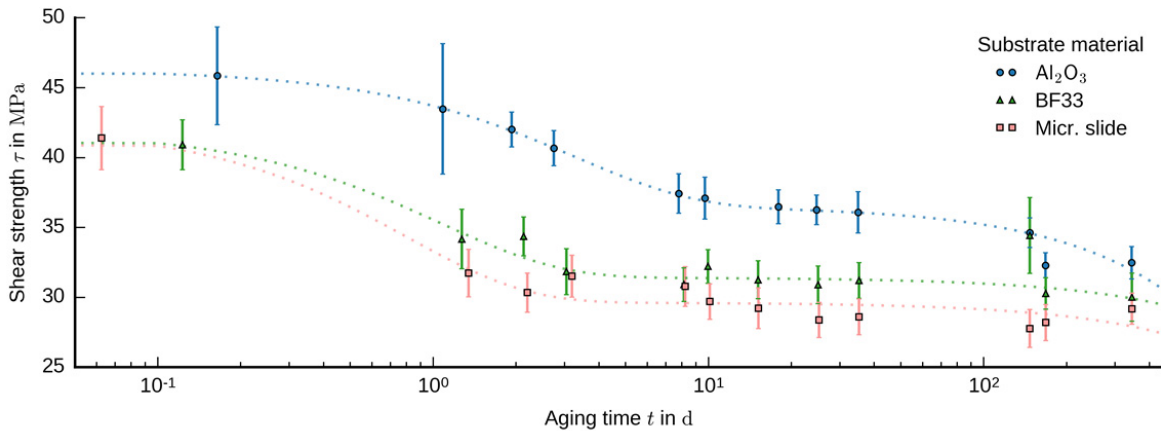


Fig. 8. Development of shear strengths of SAC305 for all examined substrate types after aging at room temperature with logarithmic time scale. The dotted lines mark fits of functions $\tau(t) = A \exp(at) + Bt + C$ to the measured data. The fitted parameters are given in table 2.

conductivity of glass ($\approx 1 \text{ W} \cdot \text{m}^{-1} \cdot \text{K}^{-1}$) leading to different cooling rates while soldering and consequently to formation of different microstructural material compositions.

Also a simple empirical model for the aging process at room temperature was derived. The aging process roughly shows an exponential behavior for $t < 20 \text{ d}$ and a linear behavior for large times. Therefore, the approach

$$\tau(t) = A \exp(at) + Bt + C \quad (1)$$

was chosen to model this behavior. Similar models have been proposed e.g. by Ma et al. (2007). The results are given in table 2. For large times $t > 30 \text{ d}$ this function can be approximated as

$$\tau(t) = Bt + C. \quad (2)$$

Consequently, B describes a long term decay of shear strength and is in the order of magnitude of $-0.01 \text{ MPa} \cdot \text{d}^{-1}$, while C is the initial value of this linear process. It must be noted, that the value of B is only a rough estimation, since the experiment has only been conducted for about 350 days.

Table 2. Measured shear strengths of the examined substrates as fitted functions $\tau(t) = A \exp(at) + Bt + C$.

Substrate material	A in MPa	a in d^{-1}	B in $\text{MPa} \cdot \text{d}^{-1}$	C in MPa
Al_2O_3	9.77	-0.31	-0.013	36.53
BF33	10.56	-0.94	-0.004	31.41
Microscope slides	12.69	-1.24	-0.005	29.63

4. Conclusion

Studying aging properties of solder has always been difficult due to the manifold possible approaches and effects. In this work, SAC305 solder was investigated for use on coated glass and ceramic substrates for the Solderjet Bumping process. Known properties and methods from analysis of the electronic industry were verified and adopted, while several special effects and needs could be described. Influences of Solderjet Bumping and shear testing parameters were examined and the method known for ball grid array shear testing was used to quantify the aging process of SAC305 solder bumps. A simple empirical, mathematical model for the shear strength has been developed to describe aging of laser-jetted SAC305 at room temperature.

Acknowledgements

The presented work was partially funded by the Federal Ministry of Education and Research (BMBF) within the initiative “Unternehmen Region – Wachstumskern Fo+” and the project “Untersuchung ultrapräziser Freiformsysteme” (FKZ: 03WKCK1B). The authors would like to thank S. Gramens and B. Zaage for support regarding specimen preparation, shear testing, and image processing.

References

- Beckert, E., Burkhardt, B., Eberhardt, R., Tünnermann, A., 2008. Solder-Bumping – a flexible Joining Approach for the Precision Assembly of optoelectronic Systems. *Micro-Assembly Technologies and Applications: Fourth International Precision Assembly Seminar 2008*, 139–147.
- Ma, H., Suhling, J. C., Zhang, Y., Lall, P., Bozack, M. J., 2007. The Influence of Elevated Temperature Aging of Reliability of Lead Free Solder Joints. *2007 Electronic Components and Technology Conference*, 653–668.
- Zhong, C. H., Yi, S., 1998. Solder joint reliability of plastic ball grid array packages. *Soldering and Surface Mount Technology*, Vol. 11, Iss. 1, 44–48.
- Amagai, M., Watanabe, M., Omiya, M., Kishimoto, K., Shibuya, T., 2002. Mechanical characterization of Sn-Ag-based lead-free solders. *Microelectronics Reliability* 42 (2002). 951–966.
- Anderson, I. E., Harringa, J. L., 2004. Elevated Temperature Aging of Solder Joints Based on Sn-Ag-Cu: Effects on Joint Microstructure and Shear Strength. *Journal of electronic materials*, Vol. 33, No. 12, 2130–2136.
- Lechovič, E., Hodúlová, E., Szewczyková, B., Kovaříková, I., Ulrich, K., 2007. Solder joint reliability. *Slovak University of Technology*, 1–8.
- Lampe, B. T., 1976. Room Temperature Aging Properties of Some Solder Alloys. *Welding Research Supplement*, 331–340.
- Chou, G. J., 2002. Microstructure Evolution of SnPb and SnAg/Cu BGA Solder Joints during Thermal Aging. *8th International Symposium on Advanced Packaging Materials*, 39–46.
- Ding, M. Z., Wai, L. C., Zhang, S., Rao, V. S., 2012. Evaluation of Laser Solder Ball Jetting for Solder Ball Attachment Process. *IEEE 14th Electronics Packaging Technology Conference*, 23–29.
- Nakamori, T., Ikeda, M., Noguchi, K., Shimizu, I., 2002. Influence of Shear Height on Shear Strength of Tin-Lead Solder Ball Bonding. *Materials Transactions*. Vol. 43, No. 8 (2002), 2130–2136.
- Chia, J. Y. H., Cotterell, B., Chai, T. C., 2006. The mechanics of the solder ball shear test and the effect of shear rate. *Material Science and Engineering A* 417, 259–274.
- Beckert, E., Oppert, T., Azdasht, G., Zakel, E., Burkhardt, T., Hornaff, M., Scheidig, I., Eberhardt, R., Tünnermann, A., Buchmann, F., 2009. Solder Jetting – A Versatile Packaging and Assembly Technology for Hybrid Photonics and Optoelectronic Systems. *42nd International Symposium on Microelectronics*, 406–412.